HHS Public Access

Author manuscript

Oncogene. Author manuscript; available in PMC 2010 October 29.

Published in final edited form as:

Oncogene. 2010 April 29; 29(17): 2517–2527. doi:10.1038/onc.2010.17.

Inhibition of Cancer Cell Proliferation and Metastasis by Insulin Receptor Downregulation

Hua Zhang[1], **Dedra H. Fagan**[2], **Xianke Zeng**[2], **Katie T. Freeman**[1], **Deepali Sachdev**[1,3], and **Douglas Yee**[1,2,3,4]

[1]Masonic Cancer Center, University of Minnesota, Minneapolis, MN, 55455, USA

[2]Department of Pharmacology, University of Minnesota, Minneapolis, MN, 55455, USA

[3]Department of Medicine, University of Minnesota, Minneapolis, MN, 55455, USA

Abstract

Insulin receptor (IR) and the type I IGF receptor (IGF1R) are structurally and functionally related. The function of IGF1R in cancer has been well documented and anti-IGF1R strategies to treat cancer have shown initial positive results. However, the role of IR in tumor biology, independent of IGF1R, is less clear. To address this issue, short hairpin RNA (shRNA) was used to specifically downregulate IR in two cancer cell lines, LCC6 and T47D. Cells with reduced IR demonstrated reduced insulin-stimulated Akt activation, without affecting IGF1R activation. Cells with reduced IR formed fewer colonies in anchorage independent conditions. LCC6 IR shRNA xenograft tumors in mice had reduced growth, angiogenesis, and lymphangiogensis compared with LCC6 wild type cells. Accordingly, LCC6 IR shRNA clones produced less HIF1α, VEGF-A, and VEGF-D. Furthermore, LCC6 IR shRNA cells formed fewer pulmonary metastases compared to LCC6 wild type cells. By *in vivo* luciferase imaging, we have shown that LCC6 IR shRNA cells have less seeding and colonization potential in the lung and liver of mice than LCC6 cells. In conclusion, downregulation of IR inhibited cancer cell proliferation, angiogenesis, lymphangiogenesis, and metastasis. Our data argue that IR should also be targeted in cancer therapy.

Keywords

Insulin receptor; angiogenesis; lymphangiogenesis; metastasis

Introduction

The insulin like growth factor (IGF)/insulin system is complex, including three ligands (insulin, IGF-I and IGF-II) and at least four receptors (insulin receptor (IR), the type I IGF

[4]Corresponding author: Douglas Yee, Masonic Cancer Center, University of Minnesota, MMC 806, 420 Delaware St SE, Minneapolis, MN, 55455, Phone: 612 626-8487, Fax: 612 626-3069, yeexx006@umn.edu.

Conflict of Interest

The authors declare no conflict of interest.

receptor (IGF1R), hybrid IR/IGF1R receptor, and the type II IGF receptor (IGF2R)). Due to differential mRNA splicing, two IR isoforms exist, IR-A and IR-B. While IGF2R does not possess kinase activity, both IGF1R and IR contain kinase domains in the β subunits. Activated receptor, by ligand binding, recruits adaptor molecules, such as insulin receptor substrate 1 and 2 (IRS-1 and IRS-2), resulting in the activation of multiple downstream signaling pathways, including the mitogen-activated protein kinase (MAPK)/Extracellular signal-regulated kinase (ERK) pathway and the phosphatidylinositol 3-kinase (PI3-K) pathway (Sachdev and Yee, 2001; Zhang and Yee, 2006).

In this complex system, IGF1R and IR interact in several important ways. First, IR and IGF1R share high homology within their kinase domains and tyrosine kinase inhibitors (TKIs) have not yet been developed that can distinguish between them. Second, IGF1R and IR form hybrid receptors by hetero-tetramerization (Kasuya *et al*., 1993). Third, while insulin binds to IR and IGF-I binds to IGF1R and the hybrid receptor, IGF-II binds to IGF1R, the hybrid receptor, and one of the IR splice isoforms, IR-A. Finally, IGF1R, IR and the hybrid receptor share similar downstream signaling adaptor molecules, such as IRS-1 and IRS-2, and signaling pathways, including MAPK and PI3-K.

IGF1R has been shown to play a critical role in cancer and several anti-IGF1R antibodies are currently in clinical trials for various types of solid tumors (Hewish *et al*., 2009; Sachdev and Yee, 2006; Weroha and Haluska, 2008). Unlike other targeted therapies, the clinical development of anti-IGF1R antibodies is further along than the TKIs (Hewish *et al*., 2009; Weroha and Haluska, 2008). There is concern that inhibition of IR by TKIs might affect glucose homeostasis and have undesirable toxicity.

The potential benefit of inhibiting IR in cancer has not been well demonstrated. In fact, recent studies on the function of insulin and the IR in cancer biology have been relatively sparse (recently reviewed by (Frasca *et al*., 2008; Pollak, 2008)). It is notable that a role for insulin was first demonstrated in the 1970s. Physiologic concentrations of insulin stimulated proliferation of breast cancer cells, whereas insulin deprivation inhibited breast cancer proliferation in a rat model (Heuson and Legros, 1972; Heuson, 1972; Osborne *et al*., 1976). Later studies have shown that MCF-7 breast cancer cells did not form tumors in a mouse model of insulin deficiency (Nandi *et al*., 1995). Furthermore, IR, especially the fetal IR-A isoform, is highly expressed in breast cancer and other malignancies (Avnet *et al*., 2009; Frasca *et al*., 2003; Zhang *et al*., 2007). Recently, it was shown that IR downregulation inhibits polyoma virus middle T antigen (PyVmT)-induced tumor growth *in vivo* (Novosyadlyy *et al*., 2009). In addition to these laboratory studies, epidemiological studies suggest that patients with hyperinsulinemia have a worse cancer outcome (Goodwin *et al*., 2002; Ma *et al*., 2008). Despite these data implicating IR in tumorigenesis, the effect of inhibiting IR alone on cancer cell biology has not been well-characterized.

In this study, we specifically downregulated the level of IR in two cancer cell lines without affecting the level or activity of IGF1R. Our data show that downregulation of IR inhibited cancer cell proliferation, angiogenesis, and lymphangiogenesis. More importantly, we show, that downregulation of IR inhibited cancer metastasis in an athymic mouse model, even in

the presence of functional IGF1R. Our data strongly argue that the IR should also be targeted in cancer therapy.

Results

IR shRNA clones had diminished IR level

In order to assess the function of the IR in cancer biology, we used shRNA technology to specifically downregulate IR levels in two cancer cell lines, LCC6 and T47D. LCC6 is a highly metastatic derivative cell line of MDA-MB-435 (Leonessa *et al*., 1996). A soluble truncated IGF1R inhibits metastasis of MDA-MB-435 cells (Dunn *et al*., 1998). Previous studies in our laboratory have shown that, in LCC6 cells, inhibition of the IGF signaling pathway by a dominant negative form of IGF1R does not affect cell proliferation, but inhibits the ability of the cells to metastasize to the lung of athymic mice (Sachdev *et al*., 2004). T47D, a breast cancer cell line, has been reported to proliferate in response to insulin (Karey and Sirbasku, 1988). In LCC6 cells, two IR shRNA clones, IR6 and IR14 were selected. Both clones had approximately 71% IR downregulation, as measured by flow cytometry (Fig. 1A). One IR shRNA clone, IR12, was also selected in T47D cells (Fig. 1B). The T47D clone had approximately 66% IR downregulation.

IR shRNA clones had diminished phosphorylation of Akt at Ser 473 in response to insulin

In order to examine the signaling profiles of LCC6 and IR shRNA clones, cellular lysates before and after insulin treatment were analyzed using a human phosphor-kinase array. This assay allowed simultaneous detection of the relative levels of forty-six phosphorylation sites from key proteins involved in cell proliferation and metastasis. In LCC6, multiple key proteins, such as p53, ERK1/2, RSK and Chk-2 (summarized in Supplemental Table 1) were constitutively phosphorylated under serum free conditions consistent with the biological aggressiveness of this cell line *in vivo*. In response to insulin for 15 minutes, only the phosphorylation of Akt at Ser 473 was induced in LCC6 cells, relative to the IR6 and IR14 cells. The constitutive phosphorylation sites observed in LCC6 were unaffected in the IR shRNA clones (Fig. 2A). Therefore, the major phosphorylation event that was altered by IR downregulation was that of Akt, a key mediator in the PI-3K pathway.

We further verified this signaling difference by immunoblotting. As shown in Fig. 2B, insulin and IGF-I treatment resulted in enhanced Ser 473 phosphorylation and activation of Akt in LCC6 cells. In contrast, IR6 or IR14 cells, which had a diminished level of IR failed to respond to insulin, as measured by the activation of Akt. IR6 and IR14 cells had intact IGF1R levels; therefore, they responded to IGF-I similar to the wild-type cells. In addition, the constitutive activation of ERK1/2 and RSK were confirmed using their phospho-specific antibodies. It is noteworthy that a pRS vector clone has similar signaling activation to wild type LCC6 (Supplemental Fig. 1), excluding the possibility that transfection and clonal selection by puromycin substantially impacted cell signaling in our settings. T47D is a less aggressive cell line, and both Akt and ERK1/2 activation are regulated by IGF-I and insulin (Byron *et al*., 2006). As shown in Fig. 2C, in response to insulin, IR12 cells have diminished activation of IRS1/2, Akt and ERK1/2 compared with pRS vector control cells. These data

suggest that downregulation of IR affected insulin signaling and decreased the phosphorylation of Akt Ser 473, while IGF-I signaling remained intact.

IR shRNA clones formed smaller colonies than wile type cells *in vitro*

Consistent with the literature, T47D cells proliferated in response to insulin in a monolayer growth assay (Fig. 3A). IR downregulation significantly decreased insulin-stimulated growth. In contrast, IGF-stimulated growth was largely unchanged in the IR clone. Furthermore, IR12 cells formed fewer and smaller colonies than T47D wild type and the vector control cells as measured by soft agar assay (Fig. 3B).

We and others have previously shown that LCC6 cells do not respond to either IGF-I or insulin in monolayer growth assays (Sachdev *et al*., 2004). Consistent with that observation, LCC6 IR6 and IR14 clones had a monolayer growth pattern similar to LCC6 wild type (data not shown). However, both IR shRNA clones formed fewer colonies than LCC6 cells and vector control cells in an anchorage-independent manner (Fig. 3C). This is consistent with our finding that insulin increased colony formation of LCC6 (data not shown).

IR shRNA clones formed smaller xenograft tumors than LCC6

To determine whether downregulation of IR inhibits tumor growth, LCC6 and the two shRNA clones were injected into the mammary fat pad of athymic mice. All cells formed xenograft tumors in athymic mice. However, IR6 and IR14 xenografts grew significantly slower than that of LCC6 cells (Fig. 4A). At the end of the experiments (28 days of tumor growth), tumor sections were analyzed by Ki-67 and TUNEL staining. As shown in Fig. 4B and 4C, LCC6 tumors had a significantly higher proliferation rate than IR6 and IR14 tumors as measured by percentage of Ki-67 staining cells. In addition, TUNEL staining of tumor sections revealed that there was a large amount of apoptosis/necrosis in the center of LCC6 tumor sections, while the apoptosis/necrosis rate in the IR6 and IR14 tumors was much less (Fig. 4D). These data indicate that LCC6 tumors were highly proliferative, highly apoptotic/necrotic, and thus had a higher turnover rate than IR6 and IR14 tumors.

IR shRNA xenografts had reduced angiogenesis and lymphangiogenesis in athymic mice

In order to assess the angiogenic and lymphangiogenic potential of LCC6 and IR shRNA xenografts, LCC6, pRS vector cells, IR shRNA clones were injected into the mammary fat pad of athymic mice to form xenograft tumors (Fig. 5A). Mice were sacrificed earlier (at day 21 of tumor growth) to examine the early development of blood vessels and lymphatic vessels in xenograft tumors. Frozen tumor sections were analyzed for the expression of CD31 and lymphatic vessel endothelial hyaluronan receptor 1 (LYVE-1), which are cell markers of blood and lymphatic vessels respectively. As shown in Fig. 5B, LCC6 or pRS vector xenografts had very well developed lymphatic vessels and blood vessels around the tumor periphery. The LCC6 wild-type tumors did not contain lymphatic vessels, but contained very dense blood vessels within the tumor. In contrast, IR shRNA clone xenografts had very poor lymphatic and blood vessel development around the tumor periphery, and they contained poorly developed blood vessels in the tumor interior. These data suggest that downregulation of IR inhibits angiogenesis and lymphangiogenesis of xenograft tumors.

IR shRNA clones had less VEGF-A and VEGF-D production than LCC6 cells

The reduced angiogenesis and lymphangiogenesis in IR shRNA xenograft tumors led us to investigate whether these cells produced less angiogenic factors, such as vascular endothelial growth factor (VEGF)-A, and lymphangiogenic factors, such as VEGF-C and VEGF-D. As shown in Fig. 6A, in response to insulin, hypoxia inducible factor 1α (HIF1α, an upstream regulator of VEGF-A expression), VEGF-A and VEGF-D mRNA levels were significantly upregulated in LCC6 wild type cells. However, insulin failed to induce changes in HIF1α, VEGF-A and VEGF-D mRNA levels in IR6 and IR14 clones. VEGF-C was at undetectable levels in this cell line (data not shown). Accordingly, we measured the level of VEGF-A in conditioned media of cultured cells (Fig. 6B). LCC6 had basal VEGF-A production, and VEGF-A levels were increased in serum conditions. Its production was further enhanced in a condition that mimics hypoxia by addition of Cobalt Chloride and 2% FBS. IR6 and IR14 cells produced a significantly lower amount of VEGF-A than LCC6 cells.

IR shRNA clones had diminished lung metastasis

It has previously been reported that LCC6 xenografts spontaneously metastasize to the lungs of athymic mice after orthotopic injection (Price, 1996; Sachdev *et al*., 2004). Mice with LCC6, IR6, or IR14 xenografts were sacrificed on the same day of tumor growth (28 days), lungs were harvested and lung sections were examined for cancer cell micrometastasis. All mice (5/5) with LCC6 xenograft tumors had numerous lung micrometastases, while 0/5 mice with IR6 or IR14 xenografts had micrometastasis, when animals were sacrificed at the same time point (data not shown). However, in this experiment, LCC6 xenografts were much larger than those of IR6 or IR14, which provided more potential seeding cells for lung metastasis. To rule out the possibility that fewer lung metastases were due to the diminished number of cells in the IR shRNA tumors, mice carrying xenografts of LCC6, IR6 or IR14 were sacrificed on different days when tumors reached approximate equal volume (~ 1000 mm^3), and lung micrometastases were examined. As shown in Fig. 7A, B, all mice (5/5) with LCC6 xenografts showed numerous lung micrometastasis, while only 1/5 mice with IR6 xenografts and 2/5 mice with IR14 xenografts showed small numbers of lung micrometastasis. These data suggest that downregulation of IR attenuated cancer cell micrometastasis in the lung.

IR shRNA clones had less seeding and colonization potential in distant organs than LCC6 cells

In order to assess the seeding and growth potential of IR shRNA clones compared with LCC6 cells, luciferase expressing LCC6 and IR shRNA clones were created. *In vitro* assays confirmed that these three cell lines expressed similar amounts of luciferase (data not shown). Equal numbers of LCC6, IR6, or IR14 cells carrying luciferase were injected into the tail vein of athymic mice. The successful delivery of the cells was confirmed by luminescent imaging after 3 hours of injection (Figure 8A, first row). Mice were examined by luminescent imaging once a week. LCC6 cells developed lung metastasis as early as 14 days post injection. At day 51, mice were first imaged alive and then sacrificed to harvest tissues. The lungs and livers of the mice were imaged (Fig. 8B). In the group of mice with

LCC6 injection, 5/5 mice had lung metastasis and 3/5 mice had liver metastasis. None of the 4 mice injected with IR6 cells had lung or liver metastasis; in mice injected with IR14 cells, 1/5 mice had a small lung metastasis and 0/5 mice had liver metastasis. In one mouse with IR6 injection, we detected two regional metastases by whole animal imaging, but neither metastasis was detected in the lung or liver imaging, suggesting they may be lymph nodes or bone metastasis. Overall, our data suggest that downregulation of IR in cancer cells inhibited their ability to seed and colonize in distant organs.

Discussion

Because the function of IGF1R in cancer biology has been well-documented, anti-IGF1R strategies are being tested clinically with antibodies and small molecule TKIs. While anti-IGF1R antibody therapies have advanced into Phase II and III clinical trials (Weroha and Haluska, 2008), small molecule TKIs against both IGF1R and IR are just completing Phase I clinical trials. To date, the TKIs have not shown specificity for IGF1R; significant inhibition of IR has also been seen with these compounds (Haluska *et al*., 2006; Ji *et al*., 2007). This raises a very intriguing question: “Is IR a valuable target in cancer cells, even though systemic inhibition may result in metabolic toxicity?” This study provides direct evidence that downregulation of IR alone inhibits cancer cell proliferation, angiogenesis, lymphangiogenesis, and metastasis, suggesting that IR should also be targeted.

Using a human phosphor-kinase profiler array, we show that in LCC6 cells, insulin stimulation resulted only in the phosphorylation of Akt at Ser 473. In the IR shRNA clone cells, the phosphorylation of Akt at this site was diminished after insulin treatment. Although we cannot rule out the possibility that other signaling pathways may be different between LCC6 and the IR shRNA clones at other time points of insulin treatment, our data imply that Akt phosphorylation and activation play a critical role in the proliferative and metastatic phenotype of LCC6 cells. These results are consistent with recent findings in transgenic mouse model systems showing a role for Akt2 in pulmonary metastasis (Dillon *et al*., 2009). As new PI3-K and Akt inhibitors are developed, the importance of insulin stimulation of this pathway in metastasis should be clarified (Maira *et al*., 2008).

Downregulation of IR inhibited the anchorage independent growth of both LCC6 and T47D cells. Furthermore, downregulation of IR in LCC6 cells inhibited xenograft tumor growth in athymic mice. All of these data demonstrate the important function of the IR in proliferation. These data are not surprising because insulin has been shown to stimulate cancer cell proliferation for over three decades (Osborne *et al*., 1976). Other evidence also supports the idea that breast tumor growth is insulin dependent and IR downregulation affects tumor growth (Heuson and Legros, 1972; Novosyadlyy *et al*., 2009). Insulin does not interact with IGF1R or the IGF1R/IR hybrids at physiological concentrations (Pandini *et al*., 1999); thus, these effects are mainly mediated by IR. It is unknown whether one isoform or both isoforms of the insulin receptor play an important role in cell proliferation. The shRNA used in this study downregulated the level of both IR isoforms; thus, we are unable to attribute our results to a specific isoform. We and others have previously shown that IR-A, which binds insulin and IGF-II, is predominantly expressed in breast cancer specimens and breast cancer cell lines (Zhang *et al*., 2007). Similarly, Avnet *et al*. has shown that IR-A is

expressed more than IR-B in human osteosarcoma samples (Avnet *et al*., 2009). These data imply that IR-A may play a more important role in tumor biology. Future studies dissecting the differences between these two isoforms are needed to shed further light on the subject.

Furthermore, our data have shown that IR regulates angiogenesis and lymphangiogenesis of cancer cells. In the literature, VEGF-A produced by cancer cells plays a significant role in angiogenesis and the metastatic dissemination of cancer cells. Our results have shown that the insulin receptor regulates VEGF-A transcription and expression, which is consistent with literature that IGF-I and insulin regulate VEGF-A through hypoxia-inducible factor-1α (HIF1α) in other types of cancer (Feldser *et al*., 1999; Fukuda *et al*., 2002; Li *et al*., 2006; Stoeltzing *et al*., 2003; Treins *et al*., 2002). Although a few reports have shown that IGF-I regulates lymphangiogenesis (Bjorndahl *et al*., 2005; Tang *et al*., 2003), we have failed to find literature regarding insulin and IR regulation of VEGF-D production and lymphangiogenesis in tumor cells. Therefore, our data suggest an important role of IR in lymphatic vessel formation in tumors.

Our data in LCC6 cells have shown that the IR, similar to IGF1R (Sachdev *et al*., 2004), regulates metastasis in invasive cancer cells. Several molecular mechanisms mediated by IR may contribute to this phenotype. First, angiogenesis is essential to the metastatic dissemination of tumor cells to distant organs (Ademuyiwa and Miller, 2008). Downregulation of IR in LCC6 cells significantly decreased the level of VEGF-A production, which may have contributed to both the reduced primary tumor proliferation at the mammary fat pad and the metastatic dissemination of tumor cells in the lung and liver of athymic mice. Second, lymphangiogenesis of IR shRNA xenograft tumors was reduced compared with wild type LCC6 xenografts. Lymphatic vessels are another pathway for tumor cells to disseminate (Eccles *et al*., 2007). Third, through direct tail vein injection methods, we have shown that IR downregulation inhibits the colonization of LCC6 cells at distant sites including the lung and liver. This may be directly linked to the function of IR in cell survival and the ability to suppress anoikis. Finally, activation of IR signaling pathways might be required for colonization in specific host tissues. While the most relevant mechanism is not certain, it is clear that IR function is necessary for spontaneous metastases.

Our studies have explored the function of IR in cancer cell proliferation, angiogenesis, lymphangiogenesis and metastasis. Yet other aspects, such as tumor metabolism, have not been directly studied in these cells. Abnormalities in glucose metabolism (Warburg effect) is an increasingly “rediscovered” hallmark of cancer (Vander Heiden *et al*., 2009). It has been shown that IR plays an important role in glucose metabolism of tumor cells (Frasca *et al*., 1999). However, a substantial portion of glucose uptake is insulin-independent (Zhang *et al*., 2007) and the direct effect of downregulation of IR on tumor metabolism needs further investigation.

Since both IGF1R and IR play important functions in cancer biology, TKIs, which do not distinguish between the two receptors, might be more beneficial to treat cancer patients if IR plays an important role in tumor cell biology. Because of the concern of diabetic side effects with IR inhibition, TKIs might be used on an intermittent schedule or in combination with other conventional or targeted therapies. Moreover, a role for IR needs to be considered in

the conduct of ongoing clinical trials. We believe that measurement of both IGF1R and IR in tumors will be needed to interpret the results of clinical trials. While IGF1R is undoubtedly a target for cancer therapy, these data, along with those from other laboratories, suggest that IR may also be a target.

Materials and Methods

Reagents

(In supplemental Materials and Methods).

Cell lines and culture

LCC6 cells were cultured in Dulbecco's modified Eagle's medium (DMEM) with 10% fetal bovine serum (FBS), 11.25 nM human insulin, 50 units/ml penicillin and 50 μg/ml streptomycin. The origin of this cell line is controversial as it has features of both melanoma and breast cancer (Chambers, 2009; Rae *et al*., 2007). T47D were cultured with Minimum Essential medium (MEM) with 5% FBS, 6 ng/L human insulin, 1% of 100X non-essential amino acids, 50 units/ml penicillin and 50 μg/ml streptomycin.

Generation of pRS vector control and IR shRNA clones in LCC6 and T47D cells

(In supplemental Materials and Methods).

Generation of luciferase expressing cell lines in LCC6 wild type and IR shRNA cells

The pSF91–LUC–EGFP vector co-expressing LucSH and enhanced green fluorescent protein (EGFP) was constructed by Dr. Shanbao Cai and kindly provided by Dr. Minghai Shao and Dr. Daniela E. Matei from Indiana University School of Medicine (Wang *et al*., 2006). This vector was transiently transfected into the Pheonix Ampho cells (Orbigen, USA) to generate retroviral particles. Retroviral particles in the supernatant were used to infect LCC6 wild type and IR shRNA cells. Cells were selected under regular culture media with100 μg/ml of zeocin (Invitrogen, USA) for three days, and then cells were sorted by GFP expression using flow cytometry. GFP positive cells were cultured in DMEM with 10% FBS, 50 units/ml penicillin and 50 μg/ml streptomycin.

Flow cytometry

Wild type cells and IR shRNA clones were incubated with a mouse IgG control antibody, or an anti-human IR antibody (83-7) in PBS/1% BSA/0.1% sodium azide (FACS buffer) for 1 hr at 4°C. Cells were washed twice, and incubated with a goat anti-mouse antibody conjugated with APC (Santa Cruz, USA) for 30 min at 4°C. Cells were washed twice, and resuspended with 400 μl FACS buffer. IR levels on cell surface were measured using a FACSCalibur flow cytometer with FL4 channel (661/16 nm Band Pass).

Cell stimulation

Cells were grown in regular growth media. Cells were washed twice with PBS and serum deprived for 24 hrs in serum free media as described previously (Sachdev *et al*., 2004).

Medium was replaced with serum free media containing IGF-I or insulin for times as indicated in figure legends.

Cell lysates

Cells were washed twice with ice-cold PBS on ice and lysed as previously described (Sachdev *et al*., 2003). Protein concentration of cell lysates was determined using the bicinchoninic acid protein assay reagent kit (Pierce).

Gel electrophoresis and immunoblotting

(In supplemental Materials and Methods).

Human phosphor-kinase array

LCC6 and IR shRNA clones cells were placed at 4×10^6 cells per 10 cm dish. The next day, cells were starved in serum free media. 24 hrs later, cells were treated with or without 20 nM insulin for 15 minutes. Cells were lysed and 300 μg of cellular lysates were used to perform the human phosphor-kinase array assay according manufacture's instruction (R&D systems, USA).

Real time RT-PCR assay

(In supplemental Materials and Methods).

VEGF-A ELISA assay

LCC6 and IR shRNA cells were plated in triplicate at 20,000 cells per well in 24-well tissue culture plates. Cells were treated in serum free media, 2% FBS, 10% FBS or 2% FBS plus 100 μM of CoCl2 for 48 hrs. The condition media was harvested and the level of VEGF in condition media was quantified using a VEGF ELISA kit from R&D systems, USA.

Monolayer growth assay

(In supplemental Materials and Methods).

Anchorage-independent growth

1 ml of 0.8% SeaPlaque-agarose (BioWhittaker, USA) in culture medium was solidified in the bottom of each well of 6 well plates. 1×10^4 cells in growth media with 2% FBS were mixed in 0.45% agarose and overlaid on the bottom agar. After 9–10 days colonies were counted under a microscope with a grid in the eyepiece. Five random selected fields were counted for each well, and the average total number of colonies from triplicate wells was shown.

Tumor growth in athymic mice

All animal studies were performed under the guideline of a University approved animal care and use protocol (Protocol No. 0511A77590 and renewed protocol No.0807A40961). 4–5 week-old female athymic mice (Foxn1nu strain from Harlan Sprague Dawley, USA) at 5 per group were injected in the 2^{nd} or 7^{th} mammary fat pad with 5×10^6 LCC6 cells. Tumor growth was measure twice each week. Tumor growth experiments were repeated three

times. At the end of experiments, mice were sacrificed and tumors were removed and fixed in formalin or frozen in O.C.T compound in liquid nitrogen. Formalin fixed tumor sections were stained with hematoxylin and eosin, Ki-67 or TUNEL respectively by the Neuropathology laboratory in the department of Laboratory Medicine and Pathology in University of Minnesota.

Tumor immunofluorescent staining

Tumor samples frozen in the O.C.T. compound were sectioned at 6 μm thickness and acetone fixed. After blocking in 0.1% BSA and 3% donkey serum in PBS (Sigma, USA), tumor sections were incubated with goat anti-mouse LYVE-1 antibody (1:100) for 30 minutes. After washing with PBS, sections were incubated with Cy™2-conjugated AffiniPure donkey anti-goat IgG (1:100) and Rat anti-mouse PE-CD31 (1:50) for 30 minutes. Finally, slides were briefly stained with DAPI and were mounted with *Prolong* Gold antifade reagent.

Confocal microscopy

Confocal laser scanning microscopy was performed with an Olympus Fluoview FV500 laser scanning confocal system using a 20X oil immersion objective. Excitation lasers and filters were as follows: DAPI, Blue Diode laser, emission 430–460 nm; Cy™2-LYVE-1, Argon laser, emission 505–525 nm; PE-CD31, Green He-Ne laser, emission LP 560 nm.

Analysis of lung micro-metastasis

Mice carrying xenograft tumors were sacrificed and lungs were fixed in formalin. Lung sections were stained with hematoxylin and eosin. Micro-metastasis were counted through the whole lung section on slides using a microscope and quantified.

In vivo and ex vivo bioluminescent imaging

1×10^6 LCC6 wild type or IR shRNA clone cells were injected into the tail vein of the 4–5 week-old female athymic mice at 5 mice per group. *In vivo* bioluminescent imaging was performed three hours after the injection, and once a week afterwards. Briefly, mice were anesthetized with 3% isoflurane and injected retroorbitally with 100 μl of 30 mg/ml D-luciferin (Caliper Life Sciences, USA) in PBS. Bioluminescence images were acquired with the IVIS Imaging System (Xenogen, USA) 2–5 minutes after injection. Analysis was performed using Living Image 2.5 software (Xenogen). For images taken at same day, the minimal and maximal counts were adjusted to be equal to reflect the difference among images. At the end point of study, 5 mice per group were imaged under 3% isofluranet. After imaging, mice were quickly sacrificed and the lungs and livers were removed and put into 6-well plates with 1 ml PBS for *ex vivo* imaging. *Ex vivo* bioluminescence images were acquired about 25–30 minutes after D-luciferin injection.

Statistical Analysis

(In supplemental Materials and Methods).

Supplementary Material

Refer to Web version on PubMed Central for supplementary material.

Acknowledgements

We are grateful to Colleen Forster for the technical service on immunohistochemistry staining of tumor and lung tissue. We thank Dr. Ilze Matise from the Masonic Cancer Center Comparative Pathology Shared Resource for valuable advice. We thank Dr. Yunfang Li and Dr. Kalpna Gupta from Masonic Cancer center for detailed protocol of LYVE-1 and CD31 staining in tumor samples. We appreciate Dr. Minghai Shao and Dr. Daniela E. Matei from Indiana University School of Medicine for providing the retroviral vector expressing luciferase. We would like to acknowledge the assistance of the Flow Cytometry Core Shared Resource of the Masonic Cancer Center. Animal imaging was performed at the Biomedical Image Processing laboratory at University of Minnesota.

Funding: This work was supported by Department of Defense Breast Cancer Research Program post-doctoral grant BC050548 to HZ, National Institutes of Health R01CA74285 to DY, and National Cancer Institute Cancer Center Support Grant P30 077598.

References

Ademuyiwa FO, Miller KD. Incorporation of antiangiogenic therapies in the treatment of metastatic breast cancer. Clin Breast Cancer. 2008; 8(Suppl 4):S151–S156. [PubMed: 19158035]

Avnet S, Sciacca L, Salerno M, Gancitano G, Cassarino MF, Longhi A, et al. Insulin receptor isoform A and insulin-like growth factor II as additional treatment targets in human osteosarcoma. Cancer Res. 2009; 69:2443–2452. [PubMed: 19258511]

Bjorndahl M, Cao R, Nissen LJ, Clasper S, Johnson LA, Xue Y, et al. Insulin-like growth factors 1 and 2 induce lymphangiogenesis in vivo. Proc Natl Acad Sci U S A. 2005; 102:15593–15598. [PubMed: 16230630]

Byron SA, Horwitz KB, Richer JK, Lange CA, Zhang X, Yee D. Insulin receptor substrates mediate distinct biological responses to insulin-like growth factor receptor activation in breast cancer cells. Br J Cancer. 2006; 95:1220–1228. [PubMed: 17043687]

Chambers AF. MDA-MB-435 and M14 cell lines: identical but not M14 melanoma? Cancer Res. 2009; 69:5292–5293. [PubMed: 19549886]

Dillon RL, Marcotte R, Hennessy BT, Woodgett JR, Mills GB, Muller WJ. Akt1 and akt2 play distinct roles in the initiation and metastatic phases of mammary tumor progression. Cancer Res. 2009; 69:5057–5064. [PubMed: 19491266]

Dunn SE, Ehrlich M, Sharp NJ, Reiss K, Solomon G, Hawkins R, et al. A dominant negative mutant of the insulin-like growth factor-I receptor inhibits the adhesion, invasion, and metastasis of breast cancer. Cancer Res. 1998; 58:3353–3361. [PubMed: 9699666]

Eccles S, Paon L, Sleeman J. Lymphatic metastasis in breast cancer: importance and new insights into cellular and molecular mechanisms. Clin Exp Metastasis. 2007; 24:619–636. [PubMed: 17985200]

Feldser D, Agani F, Iyer NV, Pak B, Ferreira G, Semenza GL. Reciprocal positive regulation of hypoxia-inducible factor 1alpha and insulin-like growth factor 2. Cancer Res. 1999; 59:3915–3918. [PubMed: 10463582]

Frasca F, Pandini G, Scalia P, Sciacca L, Mineo R, Costantino A, et al. Insulin receptor isoform A, a newly recognized, high-affinity insulin-like growth factor II receptor in fetal and cancer cells. Mol Cell Biol. 1999; 19:3278–3288. [PubMed: 10207053]

Frasca F, Pandini G, Sciacca L, Pezzino V, Squatrito S, Belfiore A, et al. The role of insulin receptors and IGF-I receptors in cancer and other diseases. Arch Physiol Biochem. 2008; 114:23–37. [PubMed: 18465356]

Frasca F, Pandini G, Vigneri R, Goldfine ID. Insulin and hybrid insulin/IGF receptors are major regulators of breast cancer cells. Breast Dis. 2003; 17:73–89. [PubMed: 15687679]

Fukuda R, Hirota K, Fan F, Jung YD, Ellis LM, Semenza GL. Insulin-like growth factor 1 induces hypoxia-inducible factor 1-mediated vascular endothelial growth factor expression, which is

dependent on MAP kinase and phosphatidylinositol 3-kinase signaling in colon cancer cells. J Biol Chem. 2002; 277:38205–38211. [PubMed: 12149254]

Goodwin PJ, Ennis M, Pritchard KI, Trudeau ME, Koo J, Madarnas Y, et al. Fasting insulin and outcome in early-stage breast cancer: results of a prospective cohort study. J Clin Oncol. 2002; 20:42–51. [PubMed: 11773152]

Haluska P, Carboni JM, Loegering DA, Lee FY, Wittman M, Saulnier MG, et al. In vitro and in vivo antitumor effects of the dual insulin-like growth factor-I/insulin receptor inhibitor, BMS-554417. Cancer Res. 2006; 66:362–371. [PubMed: 16397250]

Heuson JC, Legros N. Influence of insulin deprivation on growth of the 7,12-dimethylbenz(a)anthracene-induced mammary carcinoma in rats subjected to alloxan diabetes and food restriction. Cancer Res. 1972; 32:226–232. [PubMed: 5058183]

Heuson JC, Legros N. Influence of insulin deprivation on growth of the 7,12-dimethylbenz(a)anthracene-induced mammary carcinoma in rats subjected to alloxan diabetes and food restriction. Cancer Res. 1972; 32:226–232. [PubMed: 5058183]

Hewish M, Chau I, Cunningham D. Insulin-like growth factor 1 receptor targeted therapeutics: novel compounds and novel treatment strategies for cancer medicine. Recent Pat Anticancer Drug Discov. 2009; 4:54–72. [PubMed: 19149688]

Ji QS, Mulvihill MJ, Rosenfeld-Franklin M, Cooke A, Feng L, Mak G, et al. A novel, potent, and selective insulin-like growth factor-I receptor kinase inhibitor blocks insulin-like growth factor-I receptor signaling in vitro and inhibits insulin-like growth factor-I receptor dependent tumor growth in vivo. Mol Cancer Ther. 2007; 6:2158–2167. [PubMed: 17671083]

Karey KP, Sirbasku DA. Differential responsiveness of human breast cancer cell lines MCF-7 and T47D to growth factors and 17 beta-estradiol. Cancer Res. 1988; 48:4083–4092. [PubMed: 3289739]

Kasuya J, Paz IB, Maddux BA, Goldfine ID, Hefta SA, Fujita-Yamaguchi Y. Characterization of human placental insulin-like growth factor-I/insulin hybrid receptors by protein microsequencing and purification. Biochemistry. 1993; 32:13531–13536. [PubMed: 8257688]

Leonessa F, Green D, Licht T, Wright A, Wingate-Legette K, Lippman J, et al. MDA435/LCC6 and MDA435/LCC6MDR1: ascites models of human breast cancer. Br J Cancer. 1996; 73:154–161. [PubMed: 8546900]

Li J, Bosch-Marce M, Nanayakkara A, Savransky V, Fried SK, Semenza GL, et al. Altered metabolic responses to intermittent hypoxia in mice with partial deficiency of hypoxia-inducible factor-1alpha. Physiol Genomics. 2006; 25:450–457. [PubMed: 16507783]

Ma J, Li H, Giovannucci E, Mucci L, Qiu W, Nguyen PL, et al. Prediagnostic body-mass index, plasma C-peptide concentration, and prostate cancer-specific mortality in men with prostate cancer: a long-term survival analysis. Lancet Oncol. 2008; 9:1039–1047. [PubMed: 18835745]

Maira SM, Stauffer F, Brueggen J, Furet P, Schnell C, Fritsch C, et al. Identification and characterization of NVP-BEZ235, a new orally available dual phosphatidylinositol 3-kinase/mammalian target of rapamycin inhibitor with potent in vivo antitumor activity. Mol Cancer Ther. 2008; 7:1851–1863. [PubMed: 18606717]

Nandi S, Guzman RC, Yang J. Hormones and mammary carcinogenesis in mice, rats, and humans: a unifying hypothesis. Proc Natl Acad Sci U S A. 1995; 92:3650–3657. [PubMed: 7731959]

Novosyadlyy R, Vijayakumar A, Lann D, Fierz Y, Kurshan N, LeRoith D. Physical and functional interaction between polyoma virus middle T antigen and insulin and IGF-I receptors is required for oncogene activation and tumour initiation. Oncogene. 2009; 28:3477–3486. [PubMed: 19617901]

Osborne CK, Bolan G, Monaco ME, Lippman ME. Hormone responsive human breast cancer in long-term tissue culture: effect of insulin. Proc Natl Acad Sci U S A. 1976; 73:4536–4540. [PubMed: 1070004]

Pandini G, Vigneri R, Costantino A, Frasca F, Ippolito A, Fujita-Yamaguchi Y, et al. Insulin and insulin-like growth factor-I (IGF-I) receptor overexpression in breast cancers leads to insulin/IGF-I hybrid receptor overexpression: evidence for a second mechanism of IGF-I signaling. Clin Cancer Res. 1999; 5:1935–1944. [PubMed: 10430101]

Pollak M. Insulin and insulin-like growth factor signalling in neoplasia. Nat Rev Cancer. 2008; 8:915–928. [PubMed: 19029956]

Price JE. Metastasis from human breast cancer cell lines. Breast Cancer Res Treat. 1996; 39:93–102. [PubMed: 8738609]

Rae JM, Creighton CJ, Meck JM, Haddad BR, Johnson MD. MDA-MB-435 cells are derived from M14 melanoma cells--a loss for breast cancer, but a boon for melanoma research. Breast Cancer Res Treat. 2007; 104:13–19. [PubMed: 17004106]

Sachdev D, Hartell JS, Lee AV, Zhang X, Yee D. A dominant negative type I insulin-like growth factor receptor inhibits metastasis of human cancer cells. J Biol Chem. 2004; 279:5017–5024. [PubMed: 14615489]

Sachdev D, Li SL, Hartell JS, Fujita-Yamaguchi Y, Miller JS, Yee D. A chimeric humanized single-chain antibody against the type I insulin-like growth factor (IGF) receptor renders breast cancer cells refractory to the mitogenic effects of IGF-I. Cancer Res. 2003; 63:627–635. [PubMed: 12566306]

Sachdev D, Yee D. The IGF system and breast cancer. Endocr Relat Cancer. 2001; 8:197–209. [PubMed: 11566611]

Sachdev D, Yee D. Inhibitors of insulin-like growth factor signaling: a therapeutic approach for breast cancer. J Mammary Gland Biol Neoplasia. 2006; 11:27–39. [PubMed: 16947084]

Stoeltzing O, Liu W, Reinmuth N, Fan F, Parikh AA, Bucana CD, et al. Regulation of hypoxia-inducible factor-1alpha, vascular endothelial growth factor, and angiogenesis by an insulin-like growth factor-I receptor autocrine loop in human pancreatic cancer. Am J Pathol. 2003; 163:1001–1011. [PubMed: 12937141]

Tang Y, Zhang D, Fallavollita L, Brodt P. Vascular endothelial growth factor C expression and lymph node metastasis are regulated by the type I insulin-like growth factor receptor. Cancer Res. 2003; 63:1166–1171. [PubMed: 12649170]

Treins C, Giorgetti-Peraldi S, Murdaca J, Semenza GL, Van Obberghen E. Insulin stimulates hypoxia-inducible factor 1 through a phosphatidylinositol 3-kinase/target of rapamycin-dependent signaling pathway. J Biol Chem. 2002; 277:27975–27981. [PubMed: 12032158]

Vander, Heiden MG.; Cantley, LC.; Thompson, CB. Understanding the Warburg effect: the metabolic requirements of cell proliferation. Science. 2009; 324:1029–1033. [PubMed: 19460998]

Wang JQ, Pollok KE, Cai S, Stantz KM, Hutchins GD, Zheng QH. PET imaging and optical imaging with D-luciferin [11C]methyl ester and D-luciferin [11C]methyl ether of luciferase gene expression in tumor xenografts of living mice. Bioorg Med Chem Lett. 2006; 16:331–337. [PubMed: 16246550]

Weroha SJ, Haluska P. IGF-1 receptor inhibitors in clinical trials--early lessons. J Mammary Gland Biol Neoplasia. 2008; 13:471–483. [PubMed: 19023648]

Zhang H, Pelzer AM, Kiang DT, Yee D. Down-regulation of type I insulin-like growth factor receptor increases sensitivity of breast cancer cells to insulin. Cancer Res. 2007; 67:391–397. [PubMed: 17210722]

Zhang H, Yee D. Is the type I insulin-like growth factor receptor a therapeutic target in endometrial cancer? Clin Cancer Res. 2006; 12:6323–6325. [PubMed: 17085640]

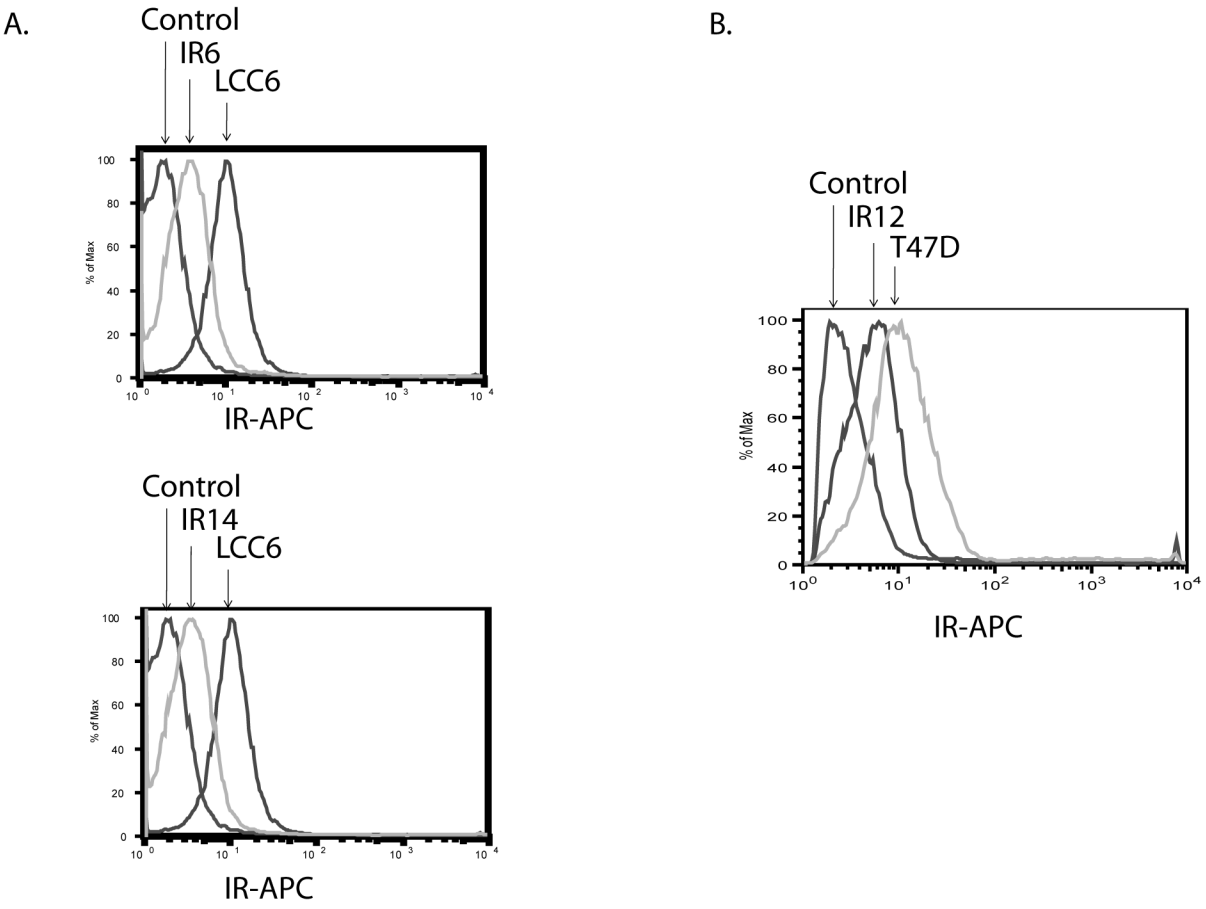

Figure 1. IR was downregulated by shRNA in LCC6 and T47D cells

Cells were stained with a mouse anti-human IR antibody, followed by a goat anti-mouse 2nd antibody conjugated with APC. The level of IR was measured by flow cytometry at channel FL4. *A*. LCC6 cells. *B*. T47D cells.

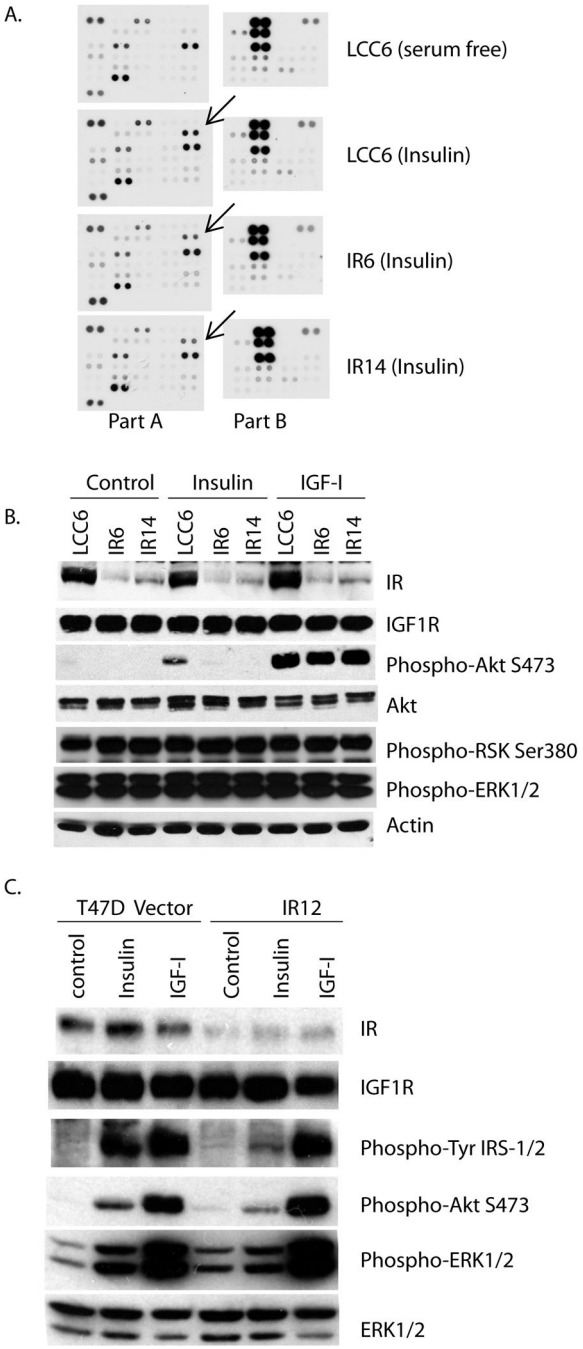

Figure 2. Downregulation of IR decreased insulin-induced signaling mainly through Akt

A. LCC6, IR6 and IR14 cells were serum starved overnight, then treated with 20 nM of insulin for 15 minutes. Cellular lysates were blotted for phosphorylation of 46 kinase phosphorylation sites. *Part A* contains 28 antibodies printed in duplicate, and *Part B* contains 18 antibodies printed in duplicate. The *arrows* point at the phosphorylation of Akt Ser 473. *B and C*. LCC6, IR6 and IR14 cells (*B*) or T47D pRS and IR12 cells (*C*) were serum starved overnight, and then treated with or without 5 nM insulin, or 5 nM IGF-I for 10 minutes. Cellular lysates were separated by SDS-PAGE, and the phosphorylation levels

of Akt at Ser473, ERK1/2 (MAPK) at Thr202/Tyr204, RSK at Ser380 and protein levels were assessed using specific antibodies by immunoblotting.

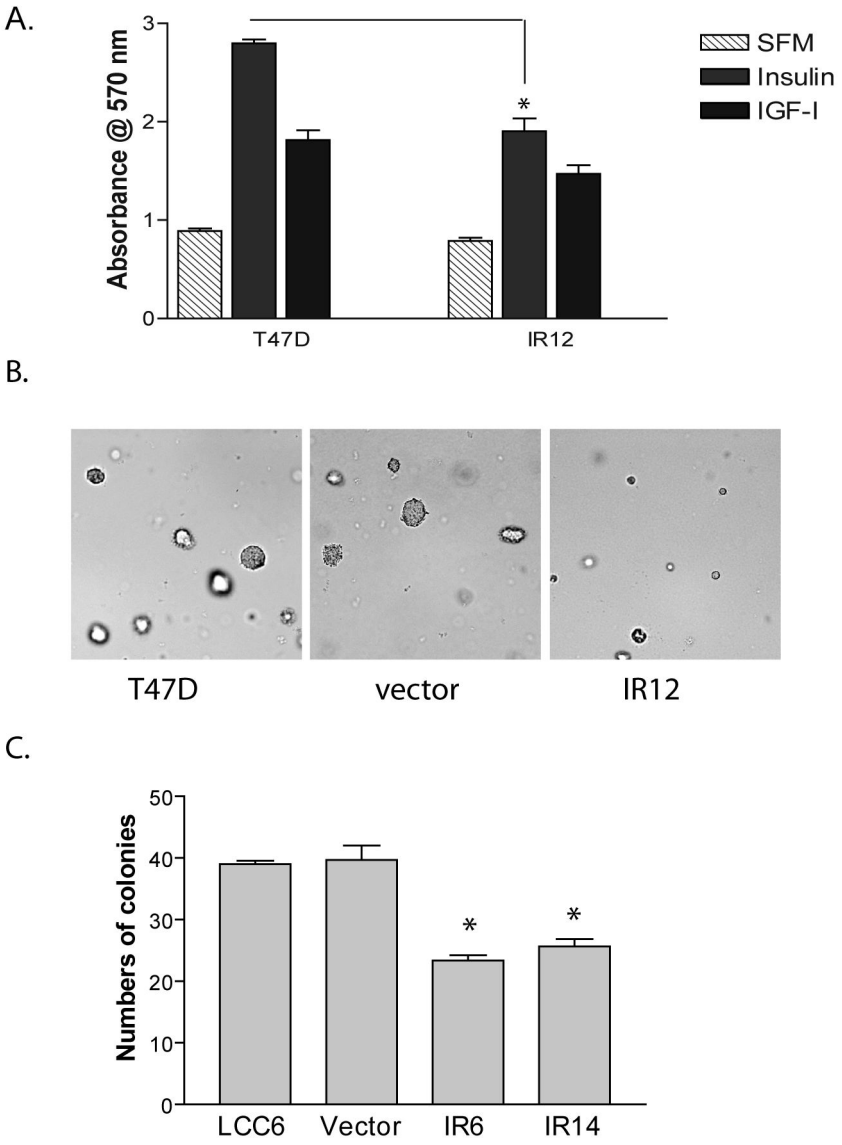

Figure 3. Downregulation of IR inhibited cell proliferation

A. T47D and IR12 clone were treated with or without insulin for 5 days. Cell numbers were estimated by MTT assay, and were shown as an absorbance at 570 nm. An unpaired *t* test was used to compare the difference between T47D and the shRNA clone. *, P<0.05. *B.* T47D cells, pRS vector cells and IR12 clone were mixed with 2% FBS in 0.45% agar and overlaid over 0.8% bottom agar. Colonies were imaged after 12 days of inoculation. Representative images were shown. *C.* The growth of LCC6 cells, pRS vector cells and two shRNA clones were measured by soft agar assay. Colonies formed were counted and averaged from 5 individual microscopic fields. The results are shown as the average number of colonies in 5 fields of three wells±S.E. The experiments were repeated three times with similar results. One way ANOVA analysis was performed to compare the difference between LCC6 and the two shRNA clones. *, P<0.05.

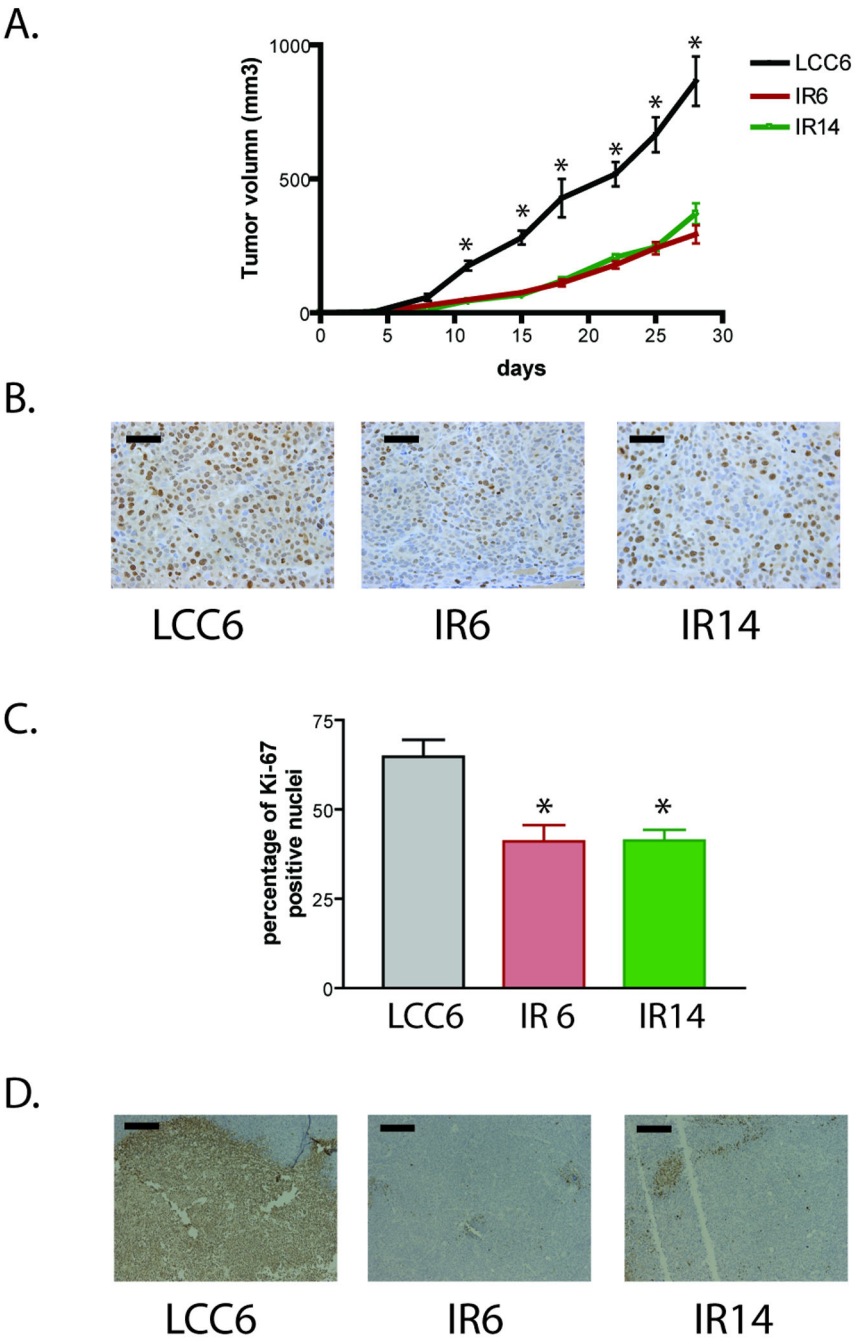

Figure 4. Downregulation of IR in LCC6 cells inhibited xenograft tumor growth in athymic mice

A. 5×10^6 LCC6 and IR shRNA clones were injected into the mammary fat pad. Tumor growth was measured twice a week and is shown as tumor volume calculated using the formula (length × width × width/2). One way ANOVA analysis was performed to compare the tumor growth within the same day. *, P<0.0001. *B.* After 28 days of tumor growth, mice were sacrificed and tumor sections were stained for Ki67. Representative images were shown. The *bar* in each image represents 50 μm in length. *C.* One way ANOVA analysis was performed to compare the percentage of positive Ki67 staining between LCC6 and the

two shRNA clones. *, P<0.05. *D*. Tumor sections were stained with TUNEL kit. Representative images were shown. The *bar* in each image represents 200 μm in length.

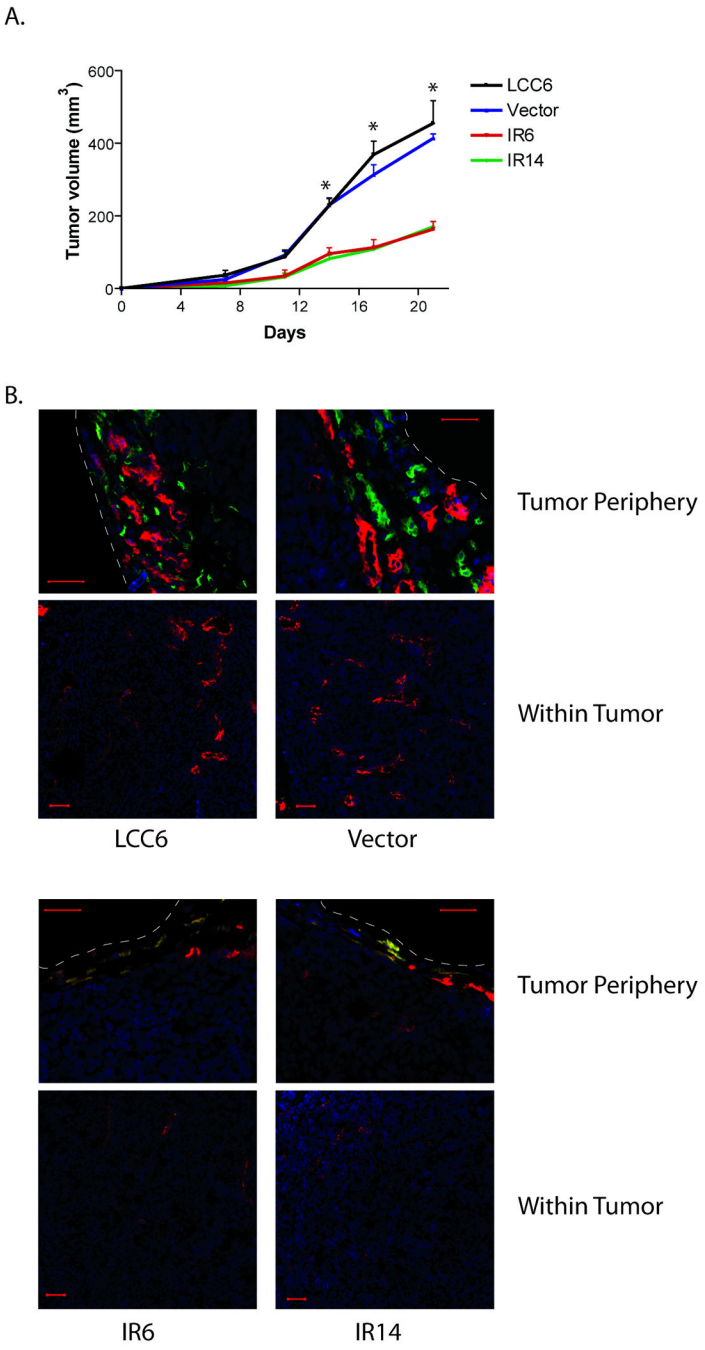

Figure 5. Downregulation of IR in LCC6 cells inhibited lymphatic and blood vessel formation of xenograft tumors in athymic mice

A. 5×10^6 LCC6, pRS vector cells, and IR shRNA clones were injected into the mammary fat pad. Tumor growth was measured twice a week and is shown as tumor volume. Mice were sacrificed after 21 days of growth. One way ANOVA analysis was performed to compare the tumor growth within the same day. *, $P<0.0001$. *B.* Tumors were frozen in OCT solution. Tumor sections were stained with LYVE-1 antibody, followed by a Cy™2 conjugated secondary antibody and PE-conjugated CD31 antibody. Finally the sections were stained for the nucleus with DAPI. Confocal microscopy was performed and representative

images of tumor periphery and tumor interiors were shown. The white dashed *lines* indicate the tumor boundary. *Blue*: DAPI; *Green*: LYVE-1; *Red*: CD31 (The *yellow* color is an overlay of *red* and *green*). The scale *bar* in the images is 50 μm.

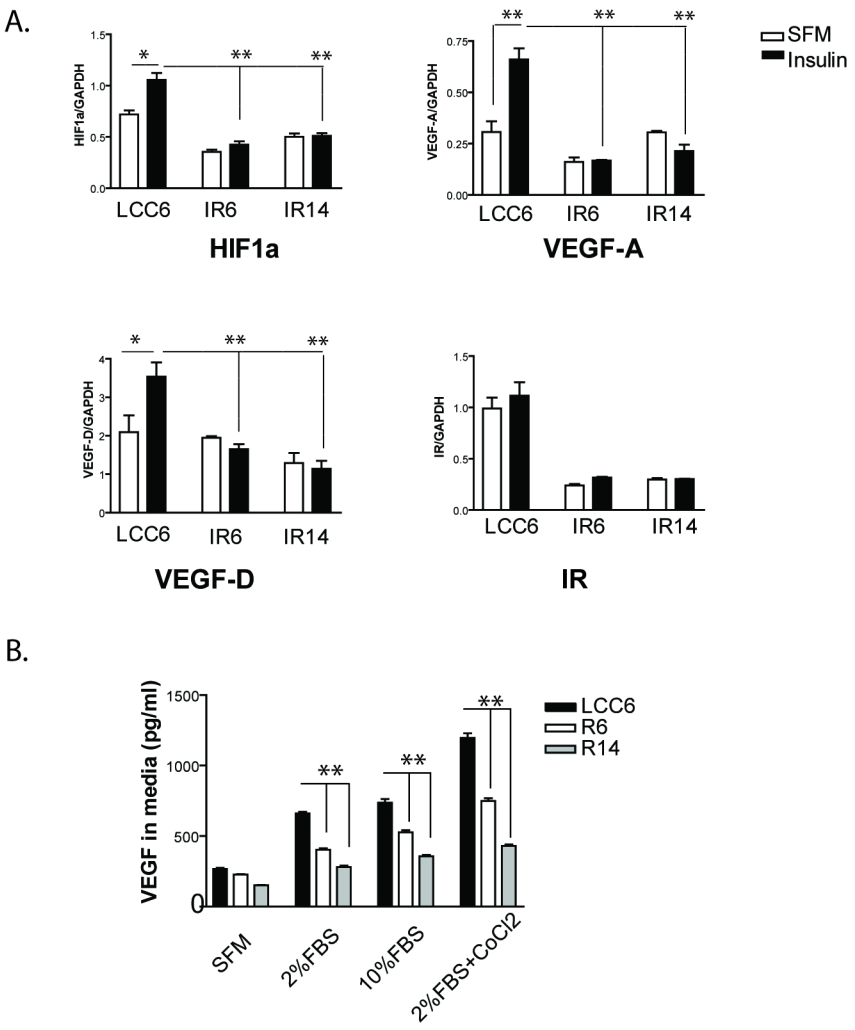

Figure 6. Insulin stimulated the expression of HIF1α, VEGF-A and VEGF-D in LCC6 cells and downregulation of IR blocked insulin-induced effects

A. Real time RT-PCR analysis. LCC6 cells and IR shRNA clones were serum starved overnight, then treated with or without 20 nM of insulin for 24 hrs. Total RNA was isolated and gene expression profiles were analyzed using real-time RT-PCRs. mRNA levels were normalized to GAPDH mRNA levels. IR mRNA levels were used as a positive control for the RT-PCR analysis. One-way ANOVA analysis was done to compare the statistical significance among different cell lines. An unpaired *t* test was used to compare the difference between two treatment conditions. *, P<0.05; **, P<0.01. *B*. LCC6 cells and IR shRNA clones were incubated in different conditions as indicated for 48 hours. VEGF-A production in condition media was quantified by ELISA. One-way ANOVA analysis was done to compare the difference within the same treatment group. **, P<0.001.

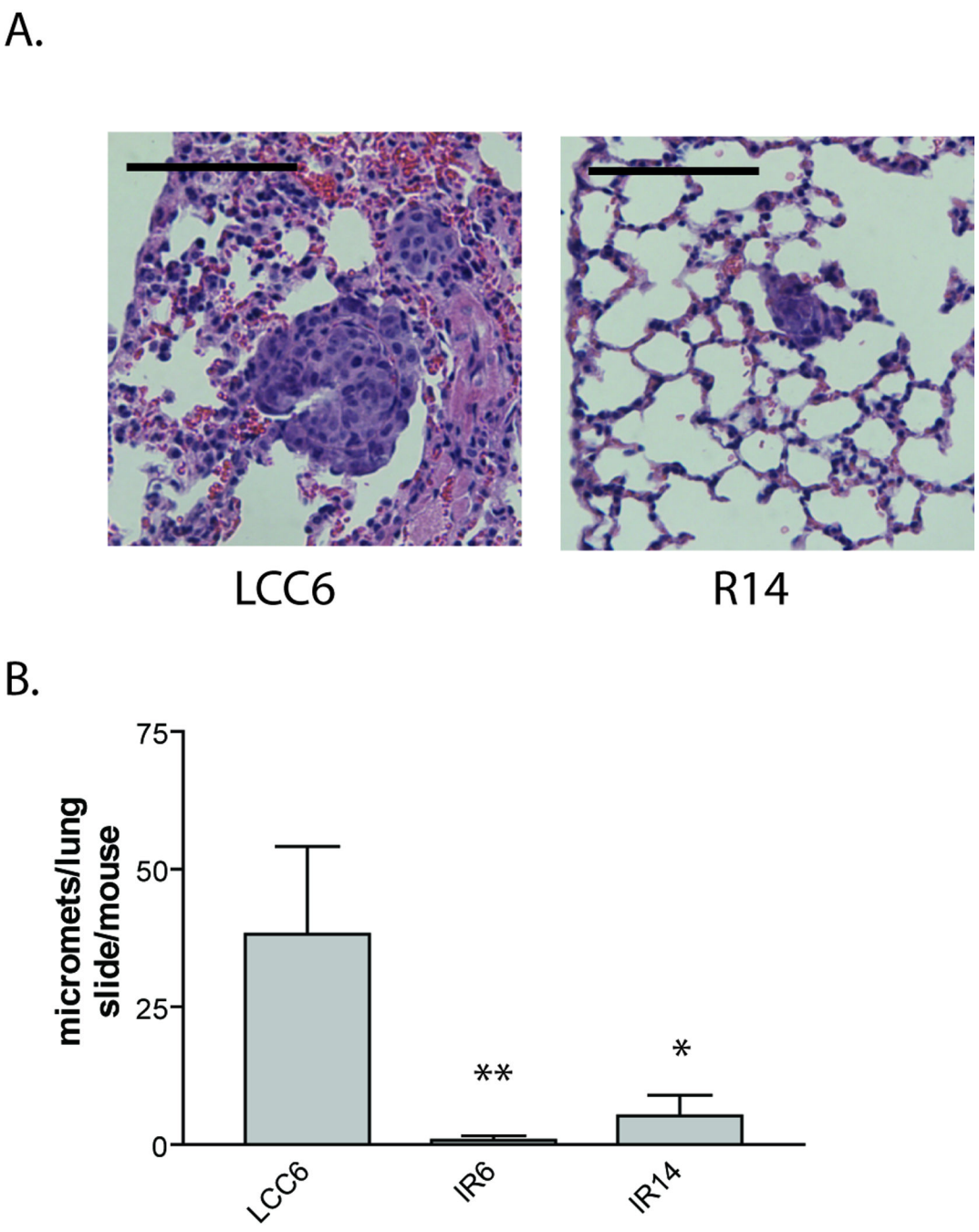

Figure 7. Downregulation of IR in LCC6 cells inhibited lung metastasis

5×10^6 LCC6 and IR shRNA clones were injected into the mammary fat pad. When tumors reached approximately 1000 mm^3 in volume, mice were sacrificed and tumor metastases were examined in the lung sections. *A*. Representative images of lung micro-metastases were shown. The *bar* in each image represents 100 μm in length. *B*. One way ANOVA analysis was performed to compare the number of micro-metastasis in the lung of mice carrying LCC6 and the two shRNA clones. *, $P<0.05$; **, $P<0.001$.

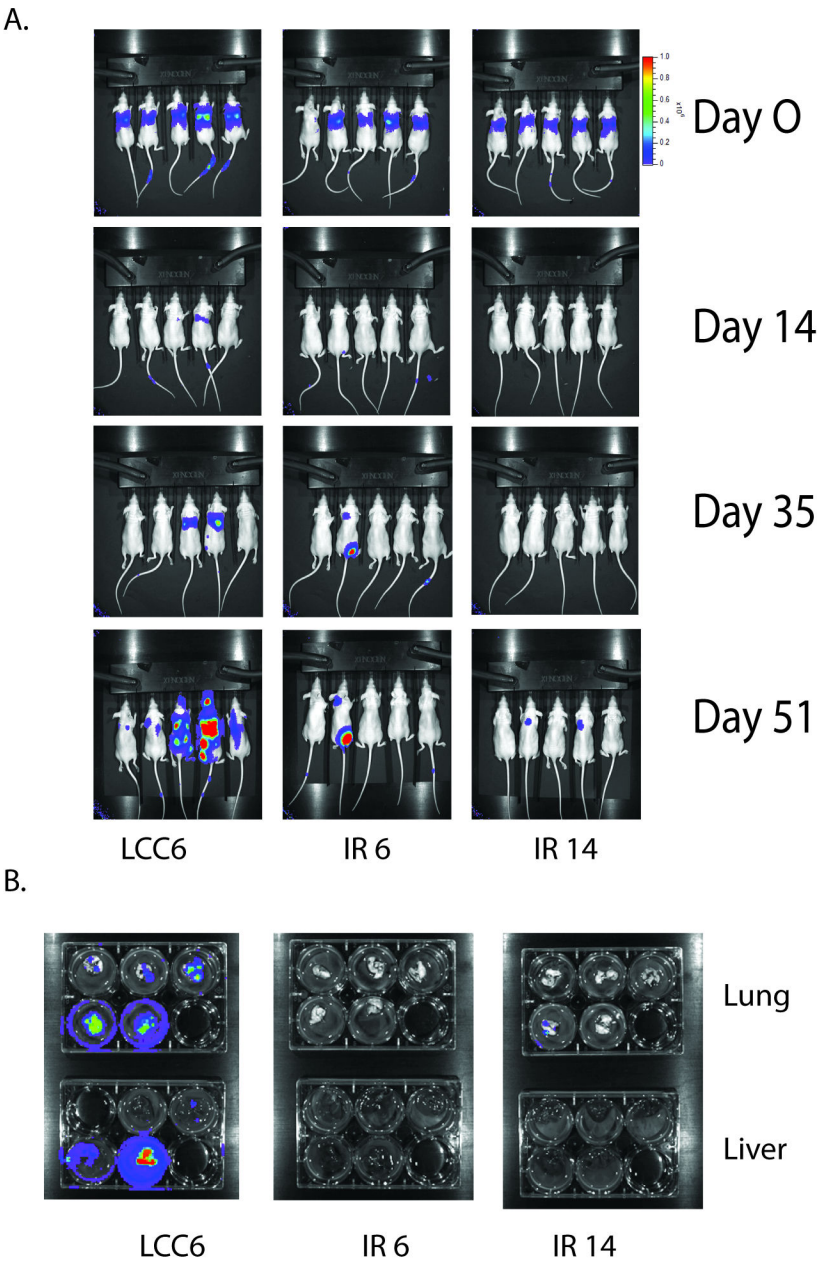

Figure 8. Downregulation of IR in LCC6 inhibited cell colonization in liver and lung of athymic mice

A. 1×10^6 cells expressing luciferase were injected into the tail vein of athymic mice. Luciferase imaging of mice whole body were performed once a week. Representative images were shown at day 0, 14, 35 and 51. *B.* At day 51, after whole body imaging, mice were sacrificed and lungs and livers were removed and placed into 6 well plates. *Ex vivo* imaging was shown.